Classes of Network Connectivity and Dynamics

OLAF SPORNS[1] AND GIULIO TONONI[2]

[1]*Department of Psychology, Indiana University Bloomington, IN 47405*

[2]*Department of Psychiatry, University of Wisconsin Madison, WI 53719. e-mail: osporns@indiana.edu*

Received August 23, 2001; accepted November 5, 2001

Many kinds of complex systems exhibit characteristic patterns of temporal correlations that emerge as the result of functional interactions within a structured network. One such complex system is the brain, composed of numerous neuronal units linked by synaptic connections. The activity of these neuronal units gives rise to dynamic states that are characterized by specific patterns of neuronal activation and co-activation. These patterns, called functional connectivity, are possible neural correlates of perceptual and cognitive processes. Which functional connectivity patterns arise depends on the anatomical structure of the underlying network, which in turn is modified by a broad range of activity-dependent processes. Given this intricate relationship between structure and function, the question of how patterns of anatomical connectivity constrain or determine dynamical patterns is of considerable theoretical importance. The present study develops computational tools to analyze networks in terms of their structure and dynamics. We identify different classes of network, including networks that are characterized by high complexity. These highly complex networks have distinct structural characteristics such as clustered connectivity and short wiring length similar to those of large-scale networks of the cerebral cortex. © 2002 Wiley Periodicals, Inc.

Key Words: complexity, connectivity, networks, covariance, information theory

Introduction

Ever since the pioneering neuroanatomical investigations conducted by Ramon y Cajal [1], the nervous system has been viewed as a network of interconnected elements. Neural networks can be described at different levels of organization, ranging from entire brain regions all the way to local circuits of individual neurons. Neuronal connections form intricate and often highly characteristic patterns that are the result of specific developmental and experience-dependent processes. As neurons communicate and interact they generate an ensemble of specific dynamical states, which can be characterized by patterns of functional interactions (functional connectivity). A wealth of experimental data suggests that perceptual and cognitive states are associated with specific patterns of functional connectivity that are generated within and between large populations of neurons in the cerebral cortex [2–5]. Clearly, anatomical patterns must play a critical role in determining which functional patterns (and thus, brain states) can and cannot occur. This article investigates the computational

principles governing the relationship between anatomical and functional connectivity.

The *anatomical connectivity* of a neuronal system is simply the set of synaptic connections linking its elements, at a given time. Elements and connections may represent individual neurons and synapses or neuronal populations and pathways. Comprehensive information on anatomical connectivity is available for the cortico-cortical and cortico-thalamic systems of the rat [6], cat [7,8], and primate [9,10], including several searchable databases on the Internet [11]. A variety of computational approaches to the analysis of neuroanatomical information have been proposed [12–16]. Several studies have focused on the analysis of connection matrices of large-scale cortical systems. Results suggest that the segregated areas of the macaque visual cortex are structurally organized into distinct subsets [13–15]. Numerous anatomical studies have also been carried out on the intrinsic connections present within single cortical areas. In many cases, these connections show patchy or mosaic termination patterns, linking neurons forming discrete domains [17,18].

The *functional connectivity* of a neuronal system comprises the pattern of temporal correlations or deviations from statistical independence between its neuronal elements that are generated by their dynamical interactions [19]. A complete description of the statistics of a neuronal system is contained in the joint probability distribution function of the system variables, with second-order effects (interactions) contained in the covariance matrix. If the joint density function is Gaussian, it is completely specified by its first- and second-order moments. These second-order moments correspond to the covariance matrix that is synonymous with its functional connectivity. Within cortical networks, two main principles of functional organization have been identified. First, cortical networks contain numerous kinds of specialized neuronal units that are functionally segregated from each other, often organized into groups or columns [20,21]. Second, in order to achieve globally coherent perceptual and cognitive states these segregated units have to be functionally integrated [22,23; see also 2–5]. The interplay between segregation and integration gives rise to distinct patterns of functional connectivity, as expressed in the structure of the covariance matrix. Can we quantify the extent to which a given neural system embodies both functional segregation and integration? Previously, we proposed a global statistical measure, called neural complexity, which is based on the pattern of functional connectivity [24,25]. This measure is low if all units within a system behave alike, for example, because of strong functional integration in the absence of functional specialization. The measure is also low if all units behave independently from each other, for example, because of the lack of any functional integration between them. However, the measure produces large positive values if a system is simultaneously segregated and integrated. In a sense, this measure expresses the amount of "interesting structure" present within a network's functional connectivity and therefore provides an indication of the network's complexity.

This article explores different classes of anatomical and functional connectivity. Our analysis centers on networks that give rise to highly complex functional connectivity. We show these networks to be organized into distinct clusters of elements, reminiscent of patterns observed within the networks of the cerebral cortex.

COMPUTATIONAL METHODS

The anatomical connectivity of a network is analyzed using methods and measures of graph theory [26,27]. The functional connectivity (covariance matrix) is obtained from the network's dynamics, and global statistical measures are defined and calculated. To identify classes of networks whose members share anatomical and functional properties, we use an evolutionary algorithm (graph selection), developed in earlier work [13,14] to guide our exploration of different network connectivties and dynamics.

Graph Theory

The structure of a given network with n units and k connections can be represented as an order-n digraph $G_{n,k}$ with n vertices and k edges (excluding self-connections, $k \leq n^2 - n$), arranged in a binary adjacency matrix $\mathbf{A}_{ij}$, corresponding to a connection matrix $\mathbf{C}_{ij}$. For a given fixed n and k there is a finite (usually very large) set of structurally distinct (non-homologous) graphs that can be generated. These graphs can be viewed as occupying discrete locations in a high-dimensional space, which we call the graph space. Rewiring a single edge within a graph moves the graph from its originaly location within this space to one that is adjacent along one of its many dimensions Repeated rewiring produces a trajectory within graph space linking successive connection patterns.

Within a digraph, a path is defined as any ordered sequence of distinct vertices and edges that links a source vertex j to a target vertex i. The length of a path is equal to the number of edges it contains. If all ordered pairs of vertices (i,j) can be linked by at least one valid path, the graph is strongly connected and contains only one component. A path linking a vertex to itself is called a cycle. The distance matrix $\mathbf{D}_{ij}$ describes the distance from vertex j to vertex i, that is, the length of the shortest valid path linking them. The average of all entries of $\mathbf{D}_{ij}$ has been called the "characteristic path length" [28,29], denoted l_{path}.

For any given vertex of a nondirected graph, the cluster index [28,29] measures how many connections exist between the vertex's neighbors, out of all possible such connections. In directed graphs, the measure is modified to

count all connections (ratio of actual/possible) within the subnetwork formed by the vertex and all of its neighbors. The cluster index of a network (f_{clust}) is calculated as the average over the cluster indices of all of the network's vertices.

Functional Dynamics

All networks considered in this article represent networks of connection pathways linking large neuronal populations composed of at least several thousand neurons. The mean activation level (fitting or population rate) of such networks can be computed as $s_i(t) = \phi[a_i(t) + N_i(t) + \omega s_i(t-1)]$ with $a_i(t)$ = synaptic inputs, $N_i(t)$ = Gaussian noise, $\omega s_i(t-1)$ = persistence, and ϕ denoting a transfer function with a saturating nonlinearity that sets an upper limit of activation [see 30]. Numerical simulations performed in this article use a hyperbolic tangent as a transfer function, linear (additive) inputs and small levels of Gaussian noise to generate spontaneous activity.

As discussed below, we find that the spontaneous activation dynamics of large-scale neural systems modeled at the population level are close to linear. This is consistent with other linear system approaches to the analysis of large-scale cortical systems [31]. Therefore, for most examples discussed in this article, we use a linear system approach, without performing nonlinear numerical simulations. Given a multidimensional Gaussian stochastic process and linear dynamics the covariance matrix $\mathbf{COV}_{ij}$ can be derived analytically from the network's connectivity matrix $\mathbf{C}_{ij}$ and the amount of injected uncorrelated noise (for details see [24,25]). Under these assumptions the covariance matrix provides a complete picture of the total set of deviations from statistical independence between all elements of the system (i.e., its functional connectivity).

Once the covariance matrix is obtained, global statistical measures can be calculated. Three such measures are used in this study: entropy (H), integration (I) and complexity (C).

For a given system X, the entropy $H(X)$ provides a measure of the system's overall degree of statistical independence. It will be maximal when its constituent units exhibit maximal statistical independence. Under stationary conditions [32,33],

$$H(X) = 0.5 \cdot \ln((2\pi e)^n |\mathbf{COV}(X)|) \qquad [1]$$

with $|\cdot|$ indicating the matrix determinant.

The integration $I(X)$ provides a measure of a system's overall deviation from statistical independence. With x_i denoting the ith individual element of the system, we obtain

$$I(X) = \Sigma_i H(x_i) - H(X) \qquad [2]$$

Note that $I(X) \geq 0$, with $I(X) = 0$ in case of complete statistical independence of all of X's constituent units.

Complexity captures the extent to which a system is both functionally segregated (small subsets of the system tend to behave independently) and functionally integrated (large subsets tend to behave coherently). A statistical measure of neural complexity $C_N(X)$ takes into account the full spectrum of subsets (k here denoting the subset size). $C_N(X)$ can be derived either from the ensemble average of integration for all subset sizes 1 to n, or (equivalently) from the ensemble average of the mutual information between subsets of a given size (ranging from 1 to $n/2$) and their complement [24,25]. $C_N(X)$ is thus defined as

$$C_N(X) = \Sigma(k/n)I(X) - \langle I(X_j^k)\rangle$$

$$= \Sigma_k \langle MI(X_j^k; X - X_j^k)\rangle$$

Another, closely related measure of complexity expresses the portion of the entropy that is accounted for by the interactions among all the components of a system. There are three mathematically equivalent expressions for this measure, called $C(X)$:

$$C(X) = H(X) - \Sigma_i H(x_i | X - x_i)$$

$$= \Sigma_i MI(x_i; X - x_i) - I(X)$$

$$= (n-1)I(X) - n\langle I(X - x_i)\rangle \qquad [3]$$

These three expressions for complexity are equivalent for all systems X, whether they are linear or nonlinear. Note that neither $C_N(X)$ nor $C(X)$ can take on negative values. $H(x_i | X - x_i)$ denotes the conditional entropy of each element x_i, given the entropy of the rest of the system $X - x_i$. To illustrate how $C(X)$ can be conceptualized, the second formulation of $C(X)$ is perhaps most useful. $C(X)$ is obtained as the difference of two terms: the sum of the mutual information between each individual element and the rest of the system minus the total amount of integration. Thus, $C(X)$ takes on large values if single elements are highly informative about the system to which they belong, while not being overly alike (as they would be if their total integration or total shared information is high). $C_N(X)$ and $C(X)$ are closely related, but not mathematically equivalent. In graphical representations [34], $C(X)$ corresponds to a specific component at level $n - 1$ of the full spectrum of ensemble averages of integration.

Graph Selection

A simple strategy for identifying distinct classes of networks would consist of searching graph space for subsets (regions) containing networks that share characteristic features, ei-

ther structural or functional. To do this systematically and in an unbiased fashion would require the examination of a very large number of networks. As n and k increase, even to moderate levels of $n = 32$ and $k = 320$ (values used in this article), the size of graph space becomes vast and unmanageable. Optimization strategies are needed to target specific regions of the space. In earlier work [13,14], we developed a computational method (called graph selection) for searching the huge space of possible connectivity patterns. The method uses global measures of functional dynamics as cost functions F and operates similar to an evolutionary algorighm:

A. An initial population of u random graphs is created, all with equal n and k.
B. Each of the graphs is "run" as a dynamical system, its covariance matrix is derived and its value of the cost function F is calculated. In case of linear dynamics, the covariance matrix is derived analytically.
C. After all members of a generation have been "run," they are ranked with respect to F. The single graph for which F is maximal is selectted. All others are eliminated.
D. The selected graph is replicated $u - 1$ times, with r of its connections rewired. The resulting u graphs constitute the next generation.
E. Steps B to D are repeated for a total of h generations. The value of h is determined by the number of generations needed for F to converge. In this article, $h = 3000$ in most cases.

Varying parameters such as u (generation size) and r (rewiring rate) yielded consistent and reliable results across multiple runs. For all simulations shown in this article, generation sizes of $u = 10$ and low rewiring rates ($r = 1$) were used. In all of the networks, every edge linking two vertices i and j has a fixed positive weight w_{ij}. It should be noted that rewiring only affects the pattern of connectivity, whereas n, k, and w_{ij} remain unchanged.

During graph selection, several constraints are applied. These constraints are motivated by a consideration of the properties of real neurobiological networks. Other domains of application may require different sets of constraints to yield realistic simulations.

A. "Saturation constraint": There is an upper bound on the total amount of input to each node i, i.e., $\Sigma_j(\text{abs}(w_{ij})) < 1.0$. This constraint reflects the limit on the number and total strength of synaptic connections or afferent fibers that a given neuron or neuronal population can support.
B. "Connectedness constraint": All graphs must remain strongly connected (i.e., any vertex can be reached from any other vertex by at least one path); no disconnection of the graph into separate components is allowed during graph selection. If such disconnection occurs, the network effectively splits into completely separate domains. In the brain, complete disconnection of parts of networks often leads to functional deficits and is therefore considered to be of negative adaptive value.
C. "Activation constraint": Variances of individual elements (i.e., the diagonal terms of the covariance matrix) are kept fixed (in this article, $v = 0.01$) by adjusting the strength of small self-inhibitory weights w_{ii} after changes in the connection pattern. This ensures that observed changes in global functional measures are due to changes in covariance and not due to changes in variance ("firing rate"). Local inhibitory circuits that act to normalize neuronal firing levels exist throughout the cortex.

CLASSES OF CONNECTIVITY AND DYNAMICS

Figure 1A shows representative examples of connection and covariance matrices for networks optimized for entropy, integration, and complexity as well as an example of a random network drawn from an initial population. All matrices are reordered using a k-means clustering algorithm operating on the covariance matrix. This algorithm places elements in close proximity that are highly correlated and show high overlap in their pattern of correlations with other elements. As expected, random networks exhibit no obvious structural or functional ordering. Networks with high entropy contain predominantly unidirectional connections and show little ordering in their covariance matrix. High integration is associated with the appearance of a single dense cluster of connections producing high cross-covariance within the cluster itself. The size of the cluster is only limited by the availability of connections. Of particular interest in this study are networks of high complexity. Such networks show connection and covariance matrices that, at first glance, appear to contain some degree of local ordering. There are several distinct groups or clusters of elements whose members show significant overlap in their correlational pattern. The vast majority of the connection pathways of highly complex networks are reciprocal. As shown in Figure 1B, each of the cost functions used in the runs (Eq. 1, 2, and 3) results in networks that show different combinations of values for integration and complexity. Networks with high integration show relatively low complexity and vice versa. This is consistent with the different demands imposed by the respective cost functions.

To test whether the linear model (used in Figure 1, A and B, and throughout the rest of the article) and the explicit nonlinear dynamical formulation of the networks (see above) yield similar results, we performed numerical simulations using a connection matrix obtained after optimizing

FIGURE 1

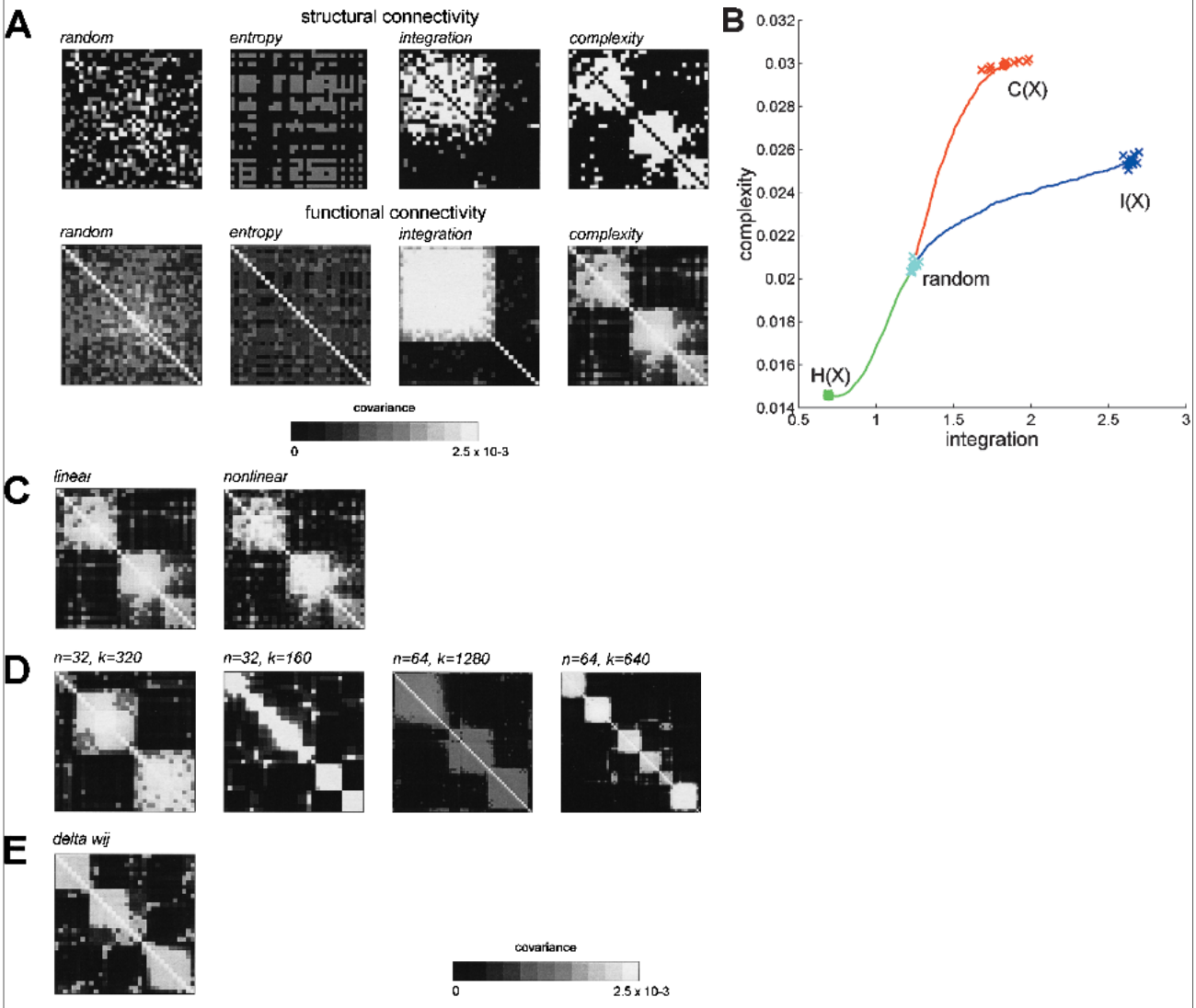

Comparison of structural and functional connectivity. (A) Examples of connection and covariance matrices for a random network (extreme left) and networks optimized for high entropy, integration, and complexity (all with $n = 32$, $k = 320$). Connection matrices (top row) show unidirectional connections in gray and bi-directional (reciprocal) connections in white. Grayscale for covariance matrices is shown at the bottom of the figure. All matrices are reordered using a *k*-means cluster algorithm (see test). (B) Average time course of integration (Eq. 2) and complexity (Eq. 3) during graph selection for entropy [$H(X)$], integration [$I(X)$], and complexity [$C(X)$]. Crosses (×) indicate final values of individual networks; a small set of random networks is also marked. (C) Comparison of covariance matrices obtained after analytical derivation under linear assumptions (left) and after numerical simulations of the nonlinear dynamical system (right). (D) Covariance matrices for networks differing in size n and connectivity k. (E) Covariance matrix obtained after graph selection by using a strategy of redistributing synaptic weight, rather than entire connections.

for complexity (Eq. 3). The covariance matrices obtained for the linear model and for the numerical simulation are highly similar (Figure 1C), providing support for the validity of the linear system approach.

When optimizing complexity, connection and covariance matrices that emerge for different network sizes, that is, different values of n and k, share common structural motifs. Larger networks organize into more numerous clusters if the average connectivity (k/n) is unchanged (Figure 1D). Lower average connectivity (lower k, with n remaining fixed) results in networks with smaller and more numerous clusters.

In all examples discussed so far, connection weights remain fixed throughout graph selection, whereas existing

connections are spatially rearranged (rewired). A more realistic way of "growing" synaptic connections is by incrementally changing their weights w_{ij} (Figure 1E). This procedure uses a selection strategy in which fractions of connection weights are redistributed throughout the network (with an upper bound on individual connections). Starting from a full ($n^2 - n$) connection matrix with weak connections, drawn at random from a normal distribution ($\mu = 0.019$, $\sigma = 0.005$), clustered connection patterns emerge, when complexity (Eq. 3) is used as a cost function. This indicates that the characteristic connectional and covariance patterns observed after redistributing fixed w_{ij}'s are not limited to that particular strategy. The rule used in Figure 1E is more realistic in that it involves small, incremental changes in synaptic weights, rather than all-or-none rewiring of connections. However, the present rule is not activity-dependent. Whether activity- (or covariance-) dependent synaptic rules can yield systematic changes in integration or complexity remains to be seen.

The eigenvalue spectrum $\{\lambda_i\}$ of the correlation matrix provides an indication of the relative amount of variance accounted for by each of the n dimensions [35]. Average eigenvalue distributions for $i = 1, \ldots, 6$ are displayed in Figure 2A. Networks with high complexity generate eigenvalue spectra with relatively large eigenvalues (λ_i significantly larger than 1) for the first two or three dimensions, indicating the existence of two or three major functional components (i.e., principal axes or components capturing most of the variance). This is in agreement with the apparent existence of local structure in their covariance matrices. Multidimensional scaling provides another way of displaying proximities between elements as revealed by the covariance matrix and their relationship to the underlying anatomy. Given that the correlation matrix is always symmetrical positive semi-definite, it can be transformed into a Euclidean dissimilarity matrix according to $\delta_{ij} = (1 - cor_{ij})^{0.5}$, with cor_{ij} indicating the value of the correlation matrix at element ij. Classical scaling (metric multidimensional scaling) in two dimensions is then performed on this dissimilarity matrix [35,36]. (Classical scaling is also referred to as principal coordinates analysis and is essentially a reformulation of principal components analysis.) After the n elements of the network are placed in two-dimensional space according to the overall similarity in their correlational pattern (i.e., their functional connectivity), the connectional pattern is superimposed to visualize the anatomical relationships between them. Figure 2B shows representative examples of such scaling plots for networks with high entropy, integration and complexity (same network as shown in Figure 1A). Not surprisingly, the random network shows no obvious spatial ordering of elements or connectivity. Networks with high entropy show very little tendency of functional overlap between any of their elements; consequently, the elements remain separated by near maximal distances and spread out evenly over all n dimensions of functional space. The two principal coordinates used in the plot capture very little (about 8%) of the total variance. High integration produces functional connectivity with a single densely connected large cluster of units surrounded by "outliers." Optimizing complexity results in two to three clusters of elements that remain interconnected. In functional space, the clusters are positioned at some distance from each other, reflecting the dissimilarity of their functional connectivity, whereas their members occupy positions in close proximity to each other, reflecting their mutual functional overlap. The two principal coordinates capture about 40–50% of the total variance. Overall, mathematical analysis of the correlation matrices obtained after optimizing complexity reveal a tendency effectively to reduce the dimensionality of functional space. As a result, functionally segregated subsets of elements emerge.

In structural terms, the "degree of separation" of individual vertices is expressed by the distance matrix $\mathbf{D}_{ij}$. Figure 3 shows examples of such distance matrices, for the same networks depicted in Figure 1A. In networks with high entropy, most vertices are separated by long distances (up to $d_{ij} \approx n/2$). This structural feature is consistent with the requirement that individual elements behave as independently as possible. Networks with high integration show small distances between vertices belonging to the central cluster and large distances between "outliers." In networks with high complexity, vertices belonging to different clusters are separated by longer distances than vertices belonging to the same cluster. Other structural characteristics that differ between different classes of networks include the characteristic path length l_{path} and the cluster index f_{clust}. A comparison of these structural measures for different network classes is shown in Figure 3B. Networks with high complexity are characterized by high values for f_{clust} and relatively low values for l_{path}.

Adjacency or connection matrices do not contain information as to the physical location of vertices in some metric space. If, for example, we want to "embed" a graph in two-dimensional space we need to assign locations to each of the vertices of the graph. How should these locations be assigned? In real neurobiological networks, it has been noted that elements appear to be arranged such that the length of the connections (the "wiring length") linking them is minimized [37,38]. Using a simple optimization algorithm, we attempted to map the vertices of a graph onto a set of locations on a two-dimensional grid such that the overall wiring length and thus the amount of "tangle" or overlap between connections is minimized. When placed optimally, networks with high complexity, but not other classes of networks, display distinct clusters of densely interconnected vertices that are linked by a smaller number of

FIGURE 2

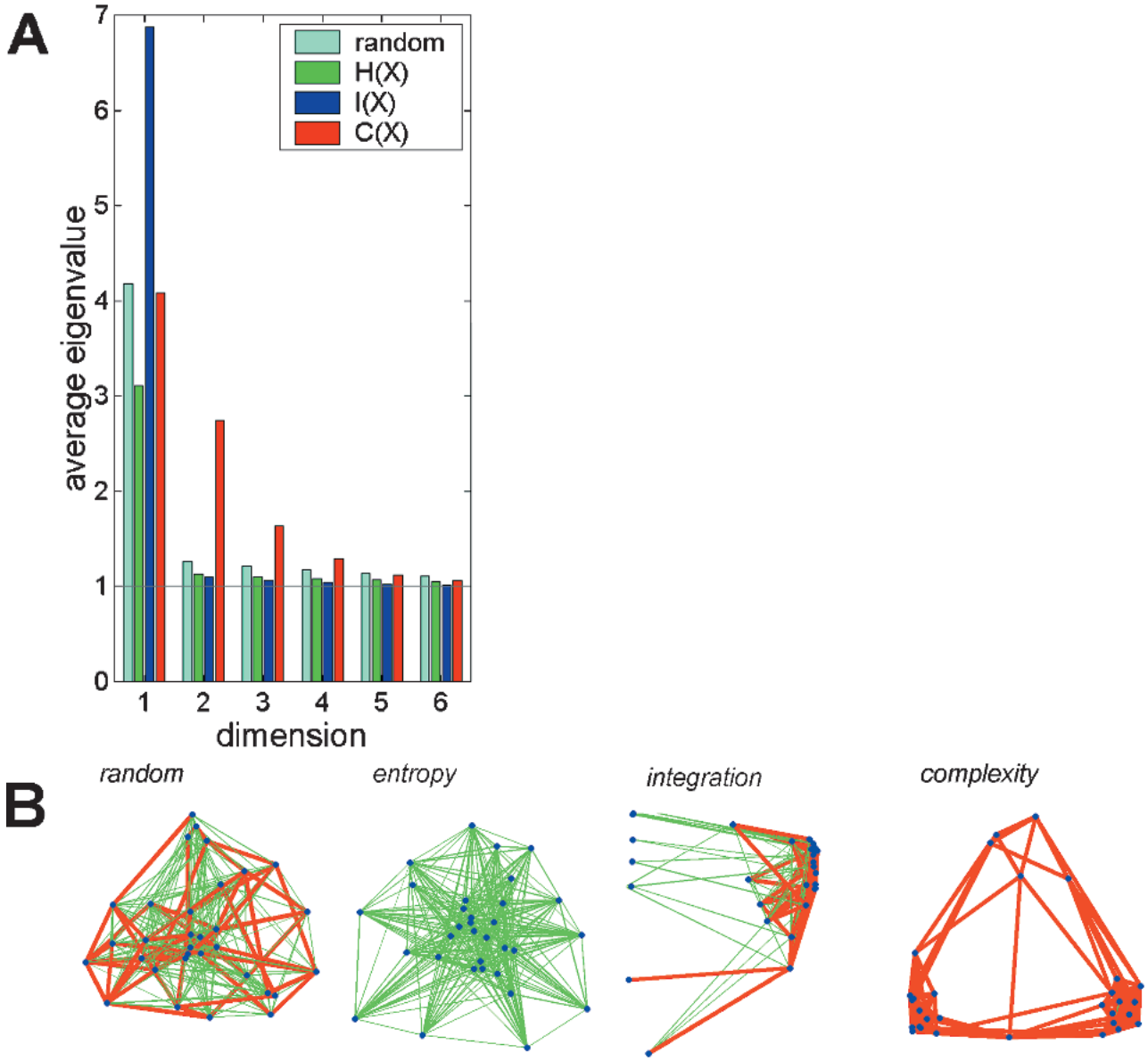

(A) Eigenvalue spectra for correlation matrices of random networks, as well as networks selected for entropy, integration, and complexity. Spectra represent averages over 10 sets of eigenvalues. Only the first six dimensions (largest eigenvalues) are shown. (B) Two-dimensional configurations obtained after metric multidimensional scaling of distance matrices derived from correlation matrices (identical to the ones displayed in Figure 1A; $n = 32$, $k = 320$). Blue dots mark locations of vertices. Red lines indicate reciprocal connections, and green lines indicate unidirectional connections. All plots are drawn at the same scale. Eigenvalue spectra of distance matrices allow the estimation of how much variance is captured by the first two principal axes; the values for the examples shown are 11.5%, 8.9%, 28.3%, and 41.0%, respectively (left to right).

long-range connections (Figure 4), a spatial arrangement reminiscent of that found in many cortical areas [17,18]. For $n = 64$, $k = 640$ and using an 8×8 grid with toroidal boundaries, the absolute minimum wiring length possible is 768 (assuming that two locations can only be linked by maximally one reciprocal connection and using a chess board distance metric). Complex networks have, on average, a wiring length of 1014 ($\sigma = 3$), which is significantly below the average value for random networks ($\mu = 1416$, $\sigma = 9$). None of the other global measures used for optimization yield such low average wiring lengths (data not shown, see Ref. [13]).

FIGURE 3

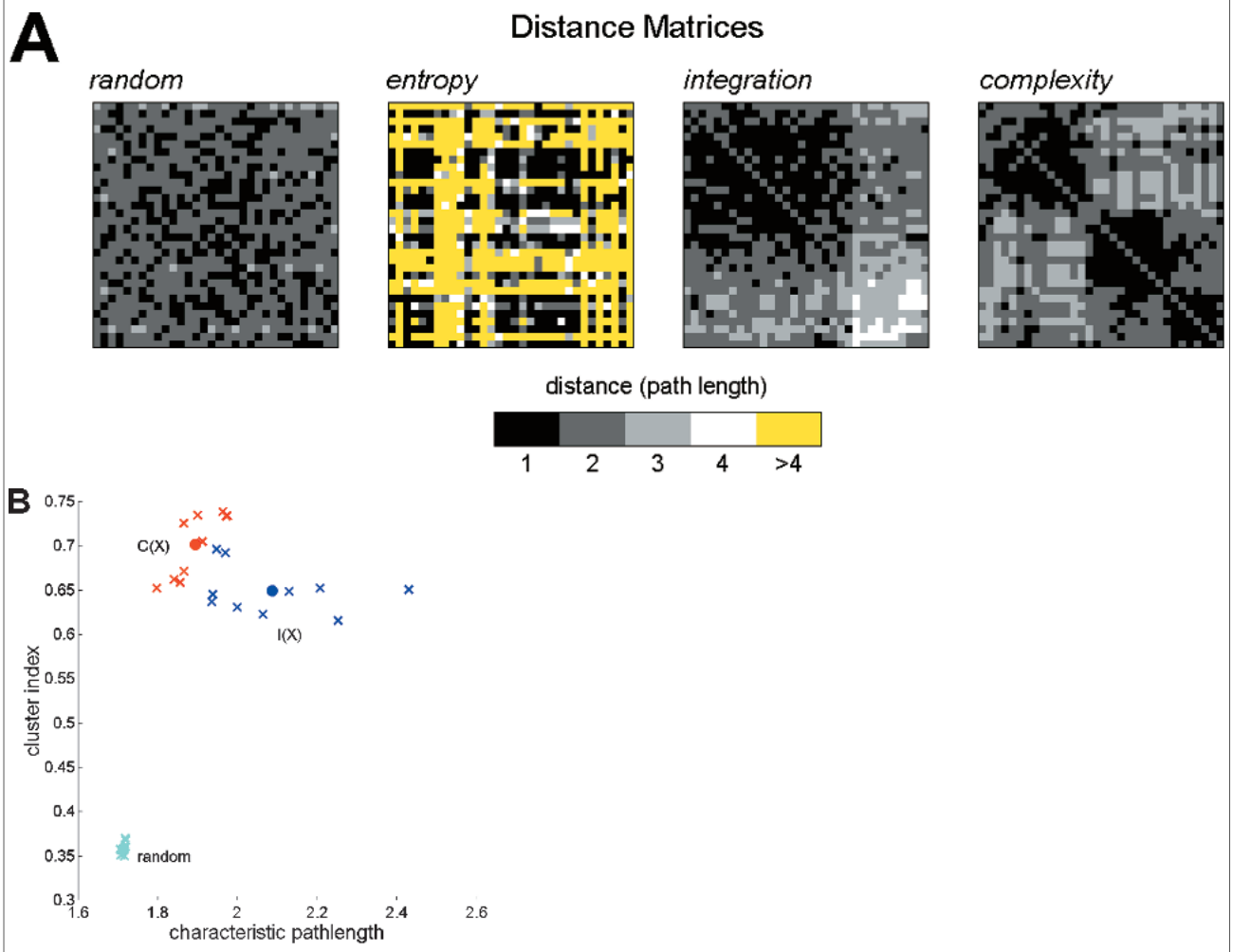

(A) Distance matrices $\mathbf{D}_{ij}$ (for corresponding connection matrices see Figure 1A), scale at bottom indicates distance between vertices j and i (black: $d_{ij} = 1$, white: $d_{ij} = 4$, yellow: $d_{ij} > 4$). (B) Plot of characteristic path length (global average of the distance matrix) and the average cluster index for examples of random networks, and networks selected for integration [$I(X)$] and complexity [$C(X)$].

CONCLUSION

Given the importance of functional connectivity patterns as neural correlates of perception, cognition, and action in higher brains [2–5], it is essential to understand how these patterns are generated and how they depend on the underlying anatomical substrate. This study aimed at identifying and characterizing distinct classes of structural and functional patterns within neuronal systems. We found that several global statistical measures of functional dynamics, when optimized, yield classes of networks that show characteristic differences in their structural and functional organization.

In a neurobiological context, patterns that result after optimization of complexity are of special interest. Complexity captures the extent to which a network is, at the same time, functionally segregated and functionally integrated. Complexity also expresses the amount of "interesting structure" that manifests itself in the system's functional connectivity. Both measures of complexity discussed in this article [$C_N(X)$ and $C(X)$] satisfy an important criterion, that of being small for both random and trivially ordered (highly regular) systems and being large for systems that contain a rich and varied set of regularities. This property of $C_N(X)$ and $C(X)$ distinguishes these measures from other complexity measures, such as dimensional complexity (correlation dimension) or algorithmic complexity (see [25] for discussion). We note that in order to obtain a system's complexity $C_N(X)$ or $C(X)$, an observer does not need to dissociate "ran-

FIGURE 4

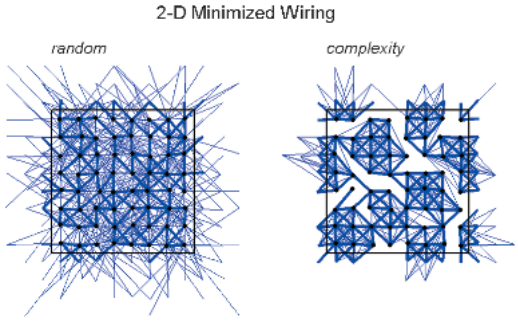

Connectivity of a random network (left) and a network selected for high complexity (right), both of size $n = 64$, $k = 640$ (see Figure 1D). Vertices (black dots) are arranged on a grid (with toroidal boundary conditions at the top and side edges) such that wiring length is minimized. Wiring length for the example shown at left (random) is 1415 and for the example shown at right (complexity) is 1012, both calculated using a chessboard distance metric. For the random network, 148 connections link vertices separated by one position in x and/or y (drawn as thick blue lines), 238 connections span two, 212 connections span three, and 42 span four positions (each drawn as thin blue lines). The corresponding numbers for the complex network are 323, 262, 55, and 0. This difference indicates that in the complex network more connections are linking neighboring vertices, resulting in shorter wiring length. Each connection is plotted only once and connections that terminate outside the central box are actually "wrapping around" the other side. Note the appearance of localized and interconnected clusters for the complex network.

dom" from nonrandom (structurally induced) components of the system's activity (cf. [39]). Furthermore, no explicit knowledge of the physical structure of the system is required. Instead, neural complexity can be applied directly to a multidimensional neuronal activation pattern, for example, a neuroimaging dataset [40]. Complexity is most usefully calculated for a neural system forming a functional cluster, a strongly interactive and coherent set of neural elements [41]

Numerous empirical studies suggest that real neurobiological networks, such as those of the cerebral cortex, combine functionally segregated and specialized neurons within globally integrated and highly interactive networks. This raises the question whether cortical neural activity is actually highly complex. When comparing networks optimized for complexity and cortical connection matrices derived from real datasets [13,14], we found that there is significant overlap in their structural and functional characteristics. For example, the cortico-cortical connection matrix of the macaque monkey visual cortex [9] give rise to highly complex neural activity patterns and is organized into distinct clusters of densely interconnected and highly interactive cortical areas [13,14]. The clustering of these areas largely corresponds to the classical distinction between ventral and dorsal streams in primate visual cortex, thus providing additional support for this distinction based on objective functional criteria.

The observation that real cortical networks are highly complex raises the question of the possible role of complexity in the origin of their connectivity patterns. There has been considerable discussion on the relationship between organizational complexity and the evolution of biological structures [e.g., 42, 43]. In this article, we generated highly complex networks by using an evolutionary optimization strategy. We note, however, that we do not consider that strategy (graph selection) to be a realistic representation of actual developmental or evolutionary mechanisms. Nonetheless, one of the effects of mechanisms operating during development and evolution may be to increase the complexity of a neural architecture by selecting for the successful integration of neural information within such architectures. Complexity, as defined in this article, captures how well a neural architecture balances the generation of specialized neural units with their functional integration to produce coherent states that can guide behavior. Evolutionary increases in complexity may simply be a manifestation of selective pressure to achieve this balance. A notable byproduct of selection for complex networks is a marked reduction in wiring length, which preserves precious "neural volume." This result highlights the important relationship between the spatial arrangement of neural components and connections and their contributions to patterns of functional connectivity.

It would be interesting to apply the optimization approach taken in this article to other network domains, such as biochemical, ecological, or social networks [44]. We would expect to find characteristic structural and functional differences across these different domains as well as some commonalities. For example, our analysis of networks modeling large-scale cortical systems yielded evidence for small-world architectures (small characteristic path length and high cluster index), whereas scale-free attributes, prominently present in much larger networks that are free from specific growth contraints such as the World Wide Web [45], appear to be absent in the cortex, at least at the level of scale studied in this article. In considering the application of complexity to other classes of networks using a different set of structural and dynamical contraints, several intriguing questions arise. If search and optimization strategies similar to the ones used in this study are used, what are the classes of connectivity and interactivity that emerge within other network domains? Do these classes have anything in common with the ones described in this article. Can optimization strategies based on global cost functions be

used to design optimal network architectures in other domains, such as communication or power networks? Does complexity, a measure of how much specialized information is integrated within a system, have applications beyond the brain? We would expect that at least some structural and functional characteristics of highly complex networks, such as their clustered connectivity and high levels of mutual information across many bipartitions, would be shared across different natural or artificial systems.

ACKNOWLEDGMENTS

We thank four anonymous reviewers for constructive comments.

REFERENCES

1. Cajal, S.R. New Ideas on the Structure of the Nervous System in Man and Vertebrates. (English translation of Les Nouvelles Idées sur la Structure des Centres Nerveux chez l'Homme et chez les Vertébrés by N. Swanson and L.W. Swanson). MIT Press: Cambridge, MA, 1990.
2. Büchel, C.; Friston, K. Assessing interactions among neuronal systems using functional neuroimaging. Neural Networks 2000, 13, 871–882.
3. McIntosh, A.R. Mapping cognition to the brain through neural interactions. Memory 1999, 7, 523–548.
4. Bressler, S.L. Large-scale cortical networks and cognition. Brain Res Rev 1995, 20, 288–304.
5. Varela, F.; Lachaux, J.-P.; Rodriguez, E.; Martinerie, J. The brainweb: Phase synchronization and large-scale integration. Nat Rev Neurosci 2001, 2, 229–239.
6. Burns, G.A.P.C.; Young, M.P. Analysis of the connectional organization of neural systems associated with the hippocampus in rats. Phil Trans R Soc Lond B 2000, 355, 55–70.
7. Scannell, J.W.; Blakemore, C.; Young, M.P. Analysis of connectivity in the cat cerebral cortex. J Neurosci 1995, 15, 1463–1483.
8. Scannell, J.W.; Burns, G.A.P.C.; Hilgetag, C.C.; O'Neil, M.A.; Young, M.P. The connectional organization of the cortico-thalamic system of the cat. Cerebral Cortex 1999, 9, 277–299.
9. Felleman, D.J.; Van Essen, D.C. Distributed hierarchical processing in the primate cerebral cortex. Cerebral Cortex 1991, 1, 1–47.
10. Young, M.P. The organization of neural systems in the primate cerebral cortex. Proc R Soc Lond B 1993, 252, 13–18.
11. Stephan, K.E.; Kamper, L.; Bozkurt, A.; Burns, G.A.P.C.; Young, M.P.; Kötter, R. CoCoMac: Advanced database methodology for complex connectivity data of the primate brain. Phil Trans R Soc Lond B 2001, 356, 1159–1189.
12. Young, M.P. Objective analysis of the topological organization of the primate cortical visual system. Nature 1992, 358, 152–155.
13. Sporns, O.; Tononi, G.; Edelman, G.M. Theoretical neuroanatomy: Relating anatomical and functional connectivity in graphs and cortical connection matrices. Cerebral Cortex 2000, 10, 127–141.
14. Sporns, O.; Tononi, G.; Edelman, G. Connectivity and complexity: The relationship between neuroanatomy and brain dynamics. Neural Networks 2000, 13, 909–922.
15. Hilgetag, C.C.; Burns, G.A.P.C.; O'Neill, M.A.; Scannell, J.W.; Young, M.P. Anatomical connectivity defines the organization of clusters of cortical areas in the macaque monkey and the cat. Phil Trans R Soc Lond B 2000, 355, 91–110.
16. Hilgetag, C.C.; Kötter, R.; Stephan, K.E.; Sporns, O. Computational methods for the analysis of brain connectivity. In: Computational Neuroanatomy: Principles and Methods. G. Ascoli, Ed., Humana Press: Totowa, NJ 2002; (in press).
17. Gilbert, C.D.; Wiesel, T.N. Columnar specificity of intrinsic horizontal and corticocortical connections in cat visual cortex. J Neurosci 1989, 9, 2432–2442.
18. Lund, J.L.; Yoshioka, T.; Levitt, J.B. Comparison of intrinsic connectivity in different areas of macaque monkey cerebral cortex. Cerebral Cortex 1993, 3, 148–162.
19. Friston, K.J. Functional and effective connectivity in neuroimaging: A synthesis. Human Brain Mapping 1994, 2, 56–78.
20. Zeki, S. Functional specialization in the visual cortex of the Rhesus monkey. Nature 1978, 274, 423–428.
21. Niebur, E.; Wörgötter, F. Design principles of columnar organization in visual cortex. Neural Comput 1994, 6, 602–624.
22. Singer, W.; Engel, A.K.; Kreiter, A.K.; Munk, M.H.J.; Neuenschwander, S.; Roelfsema, P.R. Neuronal assemblies: Necessity, signature and detectability. Trends Cognitive Sci 1997, 1, 252–261.
23. McIntosh, A.R.; Rajah, M.N.; Lobaugh, N.J. Interactions of prefrontal cortex in relation to awareness in sensory learning. Science 1999, 284, 1531–1533.
24. Tononi, G.; Sporns, O.; Edelman, G.M. A measure for brain complexity: Relating functional segregation and integration in the nervous system. Proc Nat Acad Sci USA 1994, 91, 5033–5037.
25. Tononi, G.; Edelman, G.M.; Sporns, O. Complexity and coherency: Integrating information in the brain. Trends Cognitive Sci 1998, 2, 474–484.
26. Harary, F. Graph Theory. Addison-Wesley: Reading, MA, 1969.
27. Buckley, F.; Harary, F. Distance in Graphs. Addison-Wesley: Redwood City, CA, 1990.
28. Watts, D.J.; Strogatz, S.H. Collective dynamics of 'small-world' networks. Nature 1998, 393, 440–442.
29. Watts, D.J. Small Worlds. Princeton University Press: Princeton, NJ, 1999.
30. O'Reilly, R.C.; Munakata, Y. Computational Explorations in Cognitive Neuroscience. MIT Press: Cambridge, MA, 2000.
31. McIntosh, A.R.; Gonzalez-Lima, F. Structural equation modeling and its application to network analysis in functional brain imaging. Human Brain Mapping 1994, 2, 2–22.
32. Papoulis, A. Probability, Random Variables, Stochastic Processes. McGraw-Hill: New York, 1991.
33. Jones, D.S. Elementary Information Theory. Oxford University Press: Oxford, 1979.
34. Tononi, G.; Sporns, O.; Edelman, G.M. Measures of degeneracy and redundancy in biological networks. Proc Natl Acad Sci USA 1999, 96, 3257–3262.

35. Friston, K.J.; Frith, C.D.; Fletcher, P.; Liddle, P.F.; Frackowiak, R.S.J. Functional topography: Multidimensional scaling and functional connectivity in the brain. Cerebral Cortex 1996, 6, 156–164.
36. Cox, T.F.; Cox, M.A.A. Multidimensional Scaling. Chapman & Hall: Boca Raton, FL, 2001.
37. Cherniak, C. Neural component placement. Trends Neurosci 1995, 18, 522–527.
38. Murre, J.M.J.; Sturdy, D.P.F. The connectivity of the brain: Multi-level quantitative analysis. Biol Cybernet 1995, 73, 529–545.
39. Gell-Mann, M.; Lloyd, S. Information measures, effective complexity and total information. Complexity 1996, 2, 44–52.
40. Friston, K.J.; Tononi, G.; Sporns, O.; Edelman, G.M. Characterizing the complexity of neural interactions. Human Brain Mapping 1996, 3, 302–314.
41. Tononi, G.; McIntosh, A.R.; Russell, D.P.; Edelman, G.M. Functional clustering: Identifying strongly interactive brain regions in neuroimaging data. Neuroimage 1998, 7, 133–149.
42. Schuster, P. How does complexity arise in evolution? Complexity 1996, 2, 22–30.
43. McShea, D.W. Metazoan complexity and evolution: Is there a trend? Evolution 1996, 50, 477–492.
44. Strogatz, S.H. Exploring complex networks. Nature (Lond) 2001, 410, 268–277.
45. Albert, R.; Jeong, J.; Barabasi, A.-L. The diameter of the world wide web. Nature 1999, 401, 130–131.